Macromolecules **1983,** *16,* 60-68

Polarization Mechanisms in Phase II Poly(vinylidene fluoride) Films

Brian A. Newman* and Jerry I. Scheinbeim

Rutgers, The State University of New Jersey, New Brunswick, New Jersey 08903.

Received November 17, 1981

ABSTRACT: Unoriented phase II films were poled with fields up to 3.2 MV/cm at room temperature. A determination of the piezoelectric strain coefficient provided a measure of the residual polarization achieved, while an X-ray diffraction study provided information about field-induced phase changes, which appeared to be related directly to the residual polarization. In an unoriented film, crystals make all possible orientations with respect to the poling field and different polarization mechanisms appear to depend on the crystal orientation. A number of different polarization mechanisms are discussed. A new crystal form for poly(vinylidene fluoride) (PVF_2) was observed.

Introduction

In an earlier study,[1] the effect of the poling field magnitude on crystal structure and the accompanying changes in the piezoelectric strain and stress coefficients d_{31} and e_{31} were reported for biaxially oriented poly(vinylidene fluoride) (PVF_2) films with an initial phase II (or nonpolar) crystal form. Films were poled at room temperature with fields up to 4.0 MV/cm and measurements of d_{31} and e_{31} provided a measure of the residual polarization. X-ray diffraction scans of the poled films, both in reflection and transmission mode, provided evidence for crystal structure changes occurring under field. Four distinct regions of response were observed:

(a) At low fields ($E_p < 0.6$ MV/cm) only small piezoelectric stress and strain coefficients were measured, and very little change in the X-ray diffraction scans were observed.

(b) Above a certain threshold value ($E_p > \sim 0.6$ MV/cm) and below a saturation value ($E_p < \sim 2.0$ MV/cm) both e_{31} and d_{31} increased approximately linearly with poling field. Changes in the X-ray scans (decrease to zero of the phase II (100) intensity and a slight increase in the (200) intensity) indicated that a change in crystal structure occurred in this region. The new crystal structure is now termed phase IV.[2]

(c) For fields above ~2.0 MV/cm and below ~3.6 MV/cm no further increase in d_{31} or e_{31} was produced and no further changes in the X-ray patterns were observed.

(d) For the very highest field attainable, $E_p = 4.0$ MV/cm, a further rise in the value of e_{31} was observed. X-ray diffraction showed that a second phase transition to phase I had occurred at these highest fields and was responsible for this final increase in residual polarization.

In summary, this study showed a series of phase transitions occurring under field, phase II → phase IV → phase I, giving rise to field-dependent residual polarizations in the biaxially oriented films. It is well-known that if oriented phase I films are poled, a ferroelectric switching of polar crystals gives rise to a high residual polarization, which is manifested in high piezoelectric and pyroelectric coefficients in the poled films.[3]

Table I
Unit Cell Dimensions for Different Crystal Forms of PVF_2

notations	space group	a, Å	b, Å	c, Å	ref
I, β	$Cm2m$	8.58	4.91	2.56	12, 17
II, α	$P2_1/c$	5.02	9.63	4.62	15
III, γ	$C2cm$, $\beta = 90°$	4.97	9.66	9.18	16
	Cc, $\beta = 92.9°$	4.96	9.58	9.23	16
IV, polar α	$P2cn$	4.96	9.64	4.62	2

Significant structural changes following the poling of phase II PVF_2 films have been reported by a number of workers,[4-9] many of whom advanced the hypothesis that field-induced phase transitions to polar structures (the so-called "polar α form" or in some studies also the β form) were responsible for the unexpectedly high piezoelectric activity of these films. Our study[1] showed definitely that a one-to-one correlation of the crystal structure changes with the development of residual polarization existed, to give high piezoelectric stress and strain coefficients e_{31} and d_{31}. Although phase transitions in PVF_2 in various environments have been reported, at high pressures,[10,11] under tension,[12] in films cast from different solvents,[13,14] etc., our study provided conclusive evidence that transitions from nonpolar to polar crystal structures can provide mechanisms giving rise to a residual polarization in the films. In fact, the final values obtained for the piezoelectric coefficients in the poled oriented phase II films were quite large, $d_{31} \sim 7$ pC/N and $e_{31} \sim 20$ C/m^2.

In this earlier study[1] we also included some preliminary data that showed phase transitions occurring under field for unoriented phase II PVF_2 films. It is particularly interesting to investigate unoriented films, since in this case the crystallites are disposed at widely different orientations with respect to the applied field direction. Here, we present our complete results for the unoriented films. In addition to the X-ray diffraction scans and measurements of the piezoelectric stress constant e_{31} as a function of poling field, a series of X-ray photographs was taken at different orientations with respect to the films to observe the response of crystallites at different angles with respect to the applied field. Similar X-ray photographs of the poled oriented films were taken for comparison. Measurements of the piezoelectric response were also made, since it is those crystal transformations that contribute to the polarization mechanism in which we are most interested.

Finally, it should be noted that in the presence of extremely high electric fields near the dielectric strength of the polymer, polar structures with dipole orientation in the field direction have lower free energies, and it is quite likely that these unusual conditions will predispose crystal transitions to the new structures, which perhaps cannot be produced in any other way.

Four different crystal forms have been reported for PVF_2 and their unit cell parameters and space groups are shown in Table I. Phases II, III, and IV have very similar unit cells and most reflections from phases III and IV also occur in phase II at almost the same Bragg angle. As shown in Table I, the a and b parameters reported for all three forms are very similar. For the case of phase III, the c parameter is approximately double the c parameters for phases II and

0024-9297/83/2216-0060$01.50/0

IV, so that (hkl) reflections from phase III with $l = 2n$ will occur at nearly the same Bragg angle as (hkl) reflections from phases II and IV with $l = n$. For example, the calculated (022) d spacing in form III is 3.33 Å, and the calculated (021) spacings in forms II and IV are also both 3.33 Å. Several (hkl) reflections for which $l \neq 2n$ were used in the structure determination of phase III. However, many of these could not be separated from other (hkl) reflections for which $l = 2n$ and thus coincided with phase II and phase IV reflections even for an oriented sample. The only phase III reflections that might be distinguishable from reflections from other phases in an unoriented sample are (111), (131), and (023). The structure determination for phase III was made by using an oriented sample of extremely high molecular weight synthesized by a bulk polymerization initiated by ^{60}Co γ radiation.

In the crystal structure analysis,[16] the presence of phase I, with reflections that also overlapped with phase III reflections (but not phases II or IV), was corrected for. However, the molecular conformation of phase III is reportedly completely different (T_3GT_3G') from that of phases II and IV (TGTG'). The chains are reported to pack in a statistical manner to give a polar structure.

The difference between phases II and IV is even more subtle. To date, phase IV has only been obtained by the poling of phase II films. It has almost the same unit cell dimensions and has the same molecular conformation as phase II. A statistical parallel–antiparallel packing having a polar structure was reported (phase II is nonpolar). The observed differences between phases II and IV are the electrical properties and the intensities of some reflections.

Five polarization mechanisms for PVF_2 have been already reported. The most well-known is the ferroelectric switching by 180° chain rotations (or 60° rotations) for oriented phase I crystals with the molecular chains perpendicular to the applied field.[18] A second polarizatiom mechanisms proposed is the phase II to phase IV transition for oriented phase II crystals with the molecular chains perpendicular to the applied field.[8] A third polarization mechanism is the ferroelectric switching by 180° chain rotations observed for oriented phase IV crystals with the molecular chains perpendicular to the applied field.[21] A fourth mechanism was reported to operate at very high poling fields and long poling times.[22] A fifth mechanism involves a transition to phase I.[1,23]

Polarization mechanisms in PVF_2 fall into at least two important categories: (a) ferroelectric switching in polar phases and (b) crystal transition from nonpolar to polar structures under field. In this study of phase II PVF_2 we are considering the latter type of phenomenon. In most previous studies, oriented films were used and since the applied fields during poling were perpendicular to the chain direction, only the dipole moment component perpendicular to the chain in the transformed phase is expected to be important. A study by Davis et al.[8] did include one unoriented sample poled by a corona discharge. This sample showed a partial transformation to phase I. We have seen that for the unoriented films, polarizations can be achieved that are as high as that found for the oriented films and this suggests that other polarization mechanisms can operate in which the dipole moment component along the chain is important.

In phases II, III, and IV the molecular conformations have a large moment along the chain. In all three structures the question as to the sense of packing can be raised. Three different model structures have been suggested: (a) parallel, in which the dipole moment components along the chain are all in the same direction (also referred to as the "up–up" model; this structure has a net dipole moment in the chain direction); (b) antiparallel, in which the dipole moment components along the chains alternate (also referred to as the "up–down" model; this structure has no net polarity in the chain direction), and (c) a "statistically" packed unit cell in which two chains in any given cell may be either parallel or antiparallel with equal probability (this structure will have some net polarity in the dipole direction but less than case a).

In a series of recent papers,[2,16,24] it has been suggested that for phases II, III, and IV the statistically packed model gives the best fit with the observed X-ray data. For the case of phase II, in the initial crystal structure determination,[15] it was found that the reliability for the two other possible packing cases (a) and (b) were almost identical. For the case of phase III, a parallel structure was found to give quite a low residual ($R \sim 0.18$)[16] and, according to Takahashi and Todokoro,[17] phase III does pack with the parallel structure. The model was rejected by Weinhold, Litt, and Lando[16] on the basis that several unobserved reflections were calculated to have quite large structure factors. For both phase II and phase III structure determinations, the work was carried out on unpoled films. For phase IV, the specimens were poled since this is the only method of producing this crystal structure at the present time. A statistical packing was again found to give the lowest residual.

From these considerations, we may speculate that a number of other crystal forms for PVF_2 may be possible, which, however, would only be produced by the action of a very high electric field in the appropriate direction. Crystal structures similar to the statistically packed phases II, III, or IV but with a parallel packing would give a large remnant polarization in the chain directions. We will refer to those possible structures as parallel phase II, parallel phase III, or parallel phase IV. Other structures with different unit cell dimensions may be possible either with the same $TGT\bar{G}$ conformation or with some other molecular conformation. In this respect, work with films of random orientation is very important since the applied field is at all possible orientations with respect to crystal directions. In this circumstance, phase transitions to new crystal forms would be expected.

Certain principles will govern the crystal transitions induced by field. The direction of the molecular chains would not be expected to change. The transition to a polar structure with the maximum dipole moment component in the field direction is expected. Some transitions may appear to take place by rigid-body rotations (about the chain axis) or end to end to change from antiparallel to parallel. It is assumed that a series of conformational changes (perhaps by the propagation of some defect as suggested by Lovinger[25]) can accomplish this. There may be some lattice relation between the initial and transformed crystals.

Experimental Section

Unoriented films were prepared by melting and crystallizing the oriented capacitor-grade 25-μm-thick films, which were obtained from Kureha Chemical Corp. To ensure complete melting, the polymer was heated to 230 °C for 10 min under a pressure of 1500 psi in a hot press. Crystallization at 130 °C followed by annealing at 120 °C was found to eliminate both a preferred molecular orientation and any phase I content.

The films were poled under high vacuum at room temperature with fields up to 3.2 MV/cm using a highly conducting silver paste as electrodes (which could be wiped off easily afterward). The poling time was 1 h. A thin layer of aluminum was then evaporated on the films to provide electrodes for the electrical measurements. The piezoelectric stress coefficients e_{31} and the di-

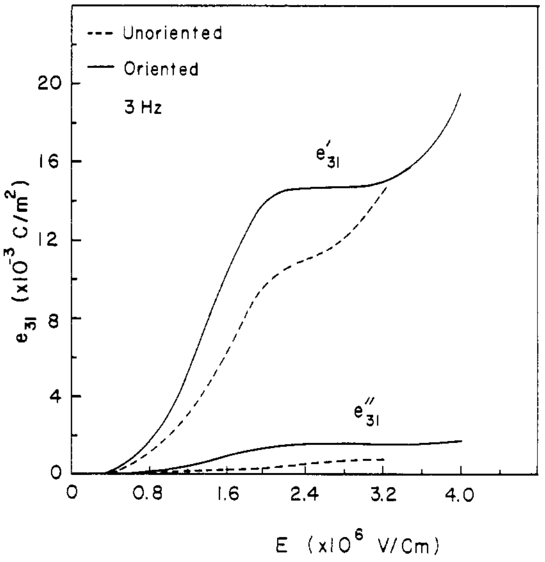

Figure 1. Comparison of piezoelectric stress coefficients e_{31} for oriented and unoriented poled PVF$_2$ films as a function of poling field.

electric constant for films poled at various fields were then measured at 3 Hz with the Toyo Seiki Piezotron.

X-ray diffraction scans in reflection and transmission modes were taken with a Phillips wide-angle diffractometer and Cu Kα radiation. X-ray patterns were also recorded on flat film, taken with the incident X-ray beam perpendicular to and parallel to the plane of the poled films.

Results

The values obtained for e_{31} for oriented films as a function of poling field are shown in Figure 1. The values obtained for e_{31} for the oriented films as a function of poling field are shown in Figure 1 for purposes of comparison. Both in-phase and out-of-phase components are included. A general similarity of behavior can be seen. Four regions of response were obtained for both oriented and unoriented films: at low fields ($E_p < 0.6$ MV/cm) only very low values of e_{31} were obtained; at higher fields ($0.6 < E_p < 2.0$ MV/cm) e_{31} increases linearly with field; a small plateau region, suggestive of the saturation of some polarization mechanism, is observed at still higher fields ($2.0 < E_p < 2.8$ MV/cm); at the highest field ($E_p = 3.2$ MV/cm) a rise in e_{31} indicates the onset of some other polarization mechanism.

The principal difference in the behavior of the two films is that the plateau region for the unoriented films is not as marked as for the oriented films, suggesting that a new polarization mechanism takes place at lower fields for the unoriented films. Following the highest poling field at 3.2 MV/cm, the piezoelectric activity in the unoriented films is as large as the value obtained for the oriented films poled at the same field. In fact, the increase of polarization with field is very high at those fields and it appears as if even higher values would have been obtained for unoriented films than for the oriented films had dielectric breakdown not intervened.

X-ray diffraction scans for the poled unoriented films in reflection and transmission modes are shown in Figures 2 and 3.

Figures 4–6 are flat-film X-ray photographs taken with the X-ray incident beam parallel to the plane of the poled film. Figure 4a, from the unpoled film, shows the complete Debye–Scherrer rings characteristic of the unoriented films. Figure 4b is a schematic diagram showing the indexed reflections. Figures 5a and 6a are the diffraction patterns corresponding to films poled at 2.4 and 3.2 MV/cm, while Figures 5b and 6b show important reflections indexed on schematic diagrams. Figure 7 shows a flat-film photograph of a film poled at 2.4 MV/cm taken with the incident X-ray beam perpendicular to the poled film.

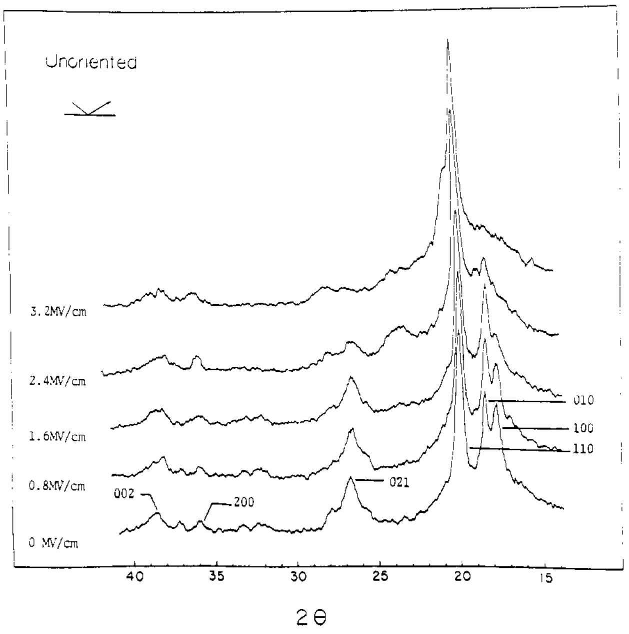

Figure 2. X-ray diffraction scans (reflection mode) of poled unoriented PVF$_2$ films.

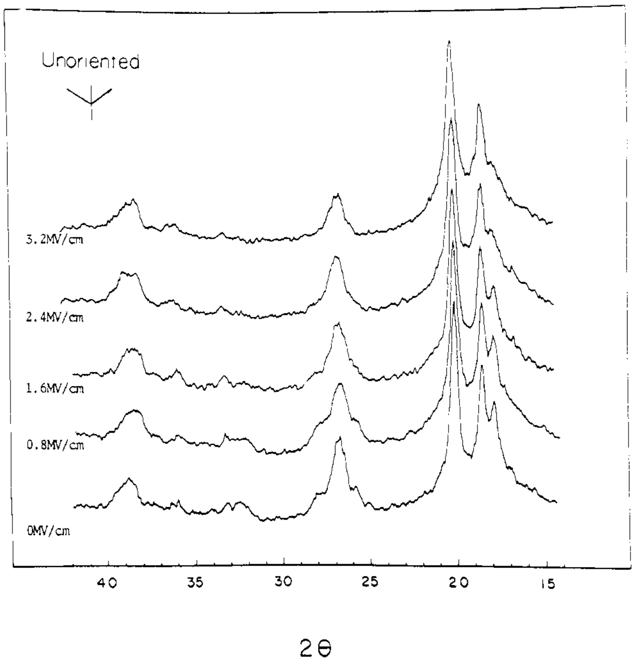

Figure 3. X-ray diffraction scans (transmission mode) of poled unoriented PVF$_2$ films.

For purposes of comparison, X-ray photographs of poled biaxially oriented phase II PVF$_2$ films were taken. Figure 8 corresponds to the unpoled oriented film taken with the incident X-ray beam in the plane of the film. Figures 9 and 10 corresponds to films poled at 2.4 and 4.0 MV/cm, respectively, with the same geometry.

In comparing the photographs with the diffraction scans, one should note that for the latter the crystals contributing to a given (*hkl*) reflection have a unique orientation; for the reflection mode the (*hkl*) direction of the set of crystals must be perpendicular to the film; for the transmission mode the (*hkl*) direction of the contributing set of crystals

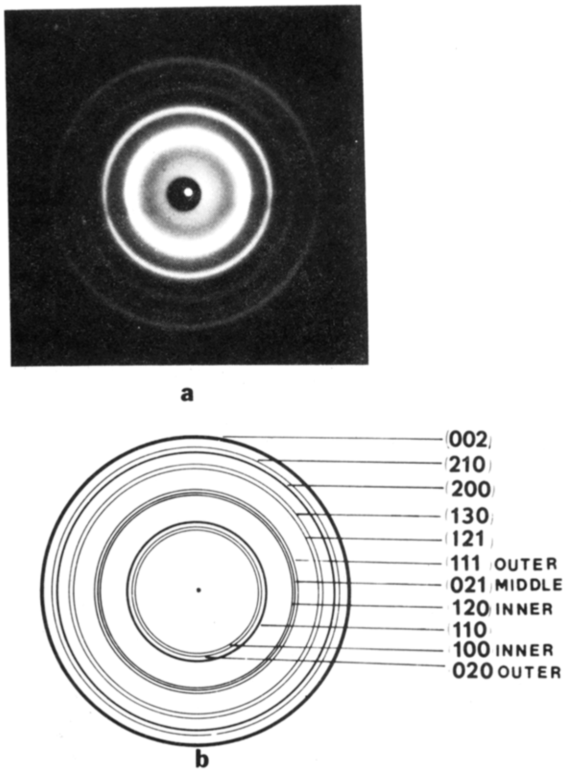

Figure 4. (a) X-ray diffraction pattern with beam parallel to plane of unpoled unoriented PVF$_2$ film. (b) Schematic illustration showing Miller indices of important reflections.

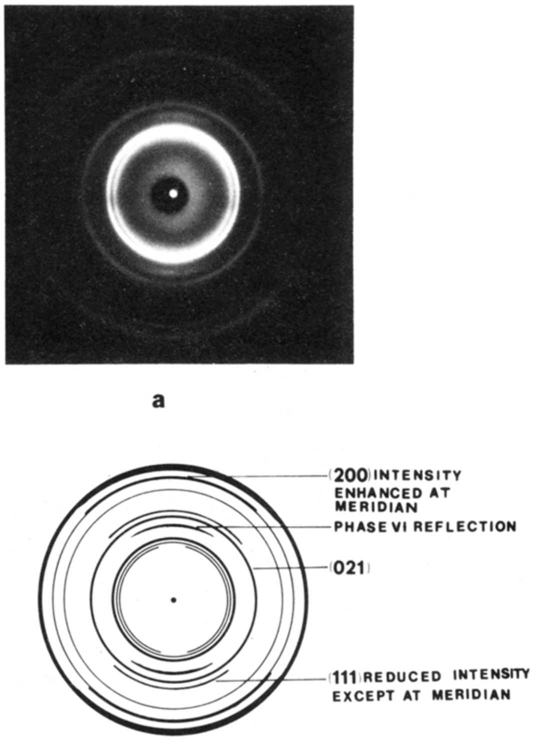

Figure 5. (a) X-ray diffraction pattern with beam parallel to plane of poled PVF$_2$ films. The poling field was 2.4 MV/cm. (b) Schematic illustration showing important reflections.

must be in the plane of the film. It is important to remember that each reflection originates from different sets of crystals making different angles with respect to the applied poling field. For the X-ray photographs, with the exception of Figure 7, the incident beam is parallel to the plane of the film. The meridional position is approximately the same as the reflection scan, except that since the film is not rotated, the crystals are rotated by the Bragg angle θ from the crystals observed in the reflection scan (for most reflections $\theta < 15\%$).

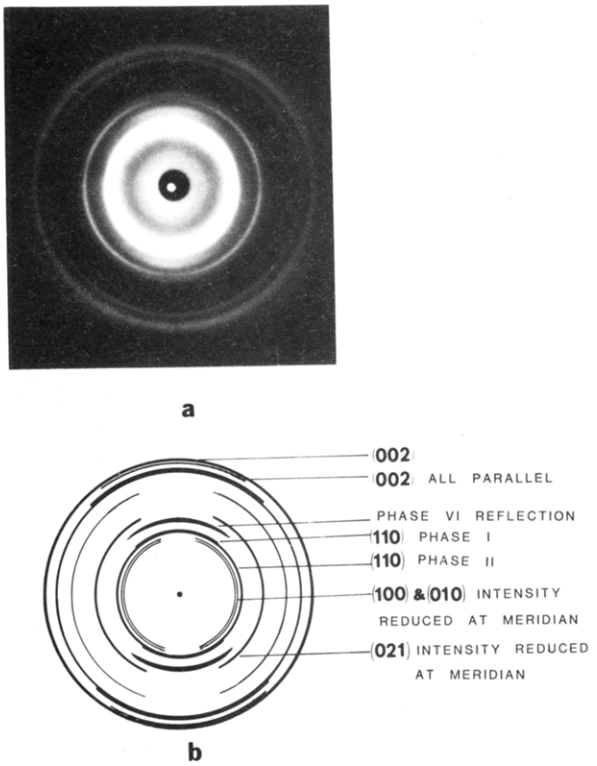

Figure 6. (a) X-ray diffraction pattern with beam parallel to plane of poled PVF$_2$ film. The poling field was 3.2 MV/cm. (b) Schematic illustration showing important reflections.

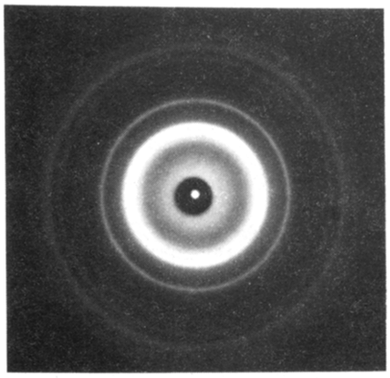

Figure 7. X-ray diffraction pattern with beam perpendicular to plane of poled PVF$_2$ film. The poling field was 2.4 MV/cm.

The interpretation of our results is complicated by the same problem that other workers have encountered, namely, the coexistence of different, but closely related crystal forms of PVF$_2$.

Discussion of the X-ray Results

Following the application of the highest poling field (3.2 MV/cm) for the unoriented films, the most intense (110) (020) reflection for phase I is seen as a shoulder on the phase II (110) peak in Figure 2. It is not seen in the diffraction scan taken in transmission (Figure 3). It can be seen in Figure 6 as a shoulder on the (110) phase II reflection, but arced in the meridional position. The phase I produced at the highest fields is clearly oriented. A transformation to oriented phase I is also observed from Figures 9 and 10 for the oriented films. A strong new reflection with a Bragg angle of 23.7° appears following poling at 2.4 MV/cm (for the unoriented films but not for

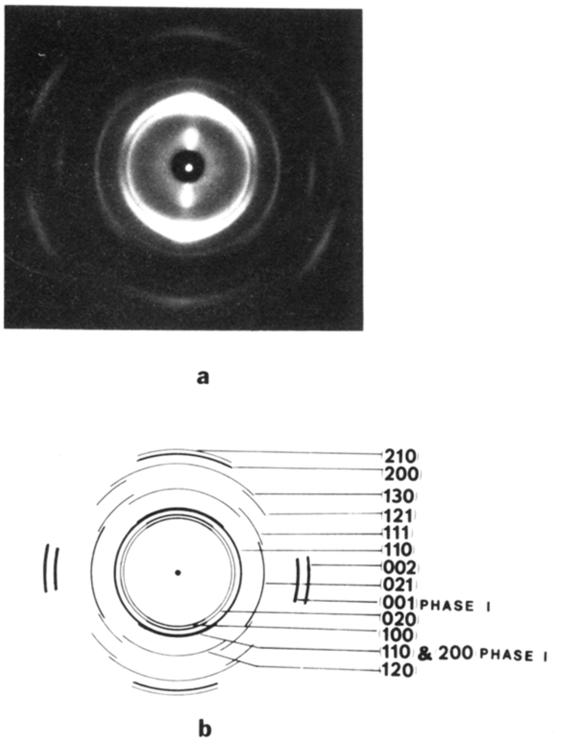

Figure 8. (a) X-ray diffraction pattern with beam parallel to plane of unpoled oriented film. (b) Schematic illustration showing important reflections.

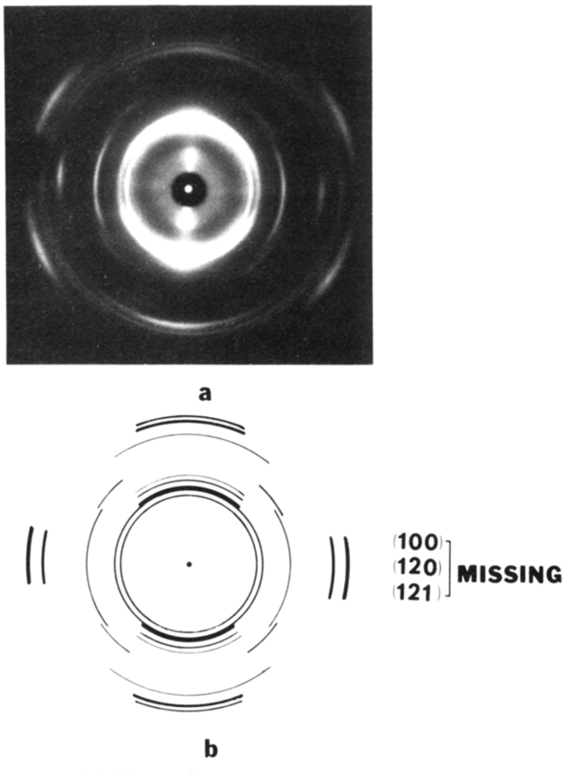

Figure 9. (a) X-ray diffraction pattern with beam parallel to plane of poled oriented film. The poling field was 2.4 MV/cm. (b) Schematic illustration showing important reflections.

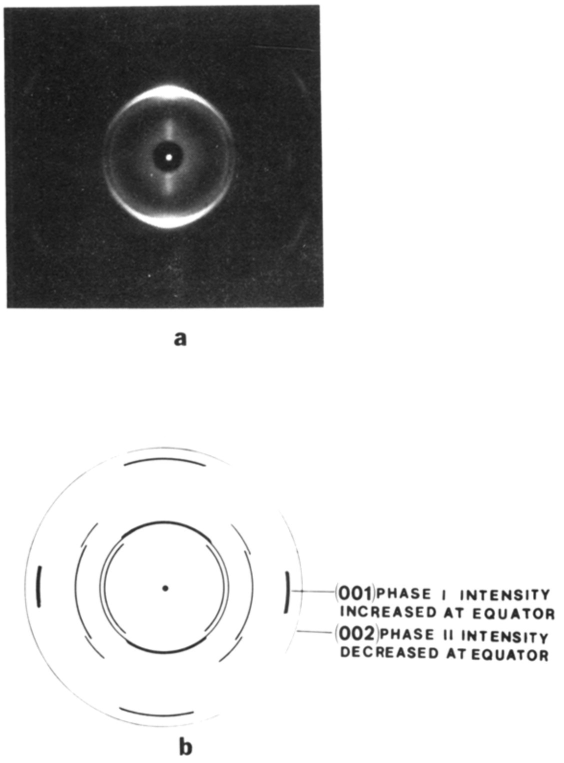

Figure 10. (a) X-ray diffraction pattern with beam parallel to plane of poled oriented films. The poling field was 4.0 MV/cm. (b) Schematic illustration showing important reflections.

the oriented films), which can be seen in the reflection scan shown in Figure 2. It is not seen in the transmission scan in Figure 3, and it is seen as an arc around the meridian in Figure 5. This reflection cannot be identified with any of the four known phases (I, II, III, or IV) even if different packing senses (for example, the antiparallel packing of $T_3GT_3\bar{G}$ chains into the phase III unit cell proposed by Lovinger as possible phase V) or defect structures permit reflections that are normally forbidden. This imples either that one of the previous structure determinations is incorrect or, more likely, that under these poling conditions, we have produced a new phase of PVF_2, which, following the recently established nomenclature, could be labeled phase VI. Figure 5 clearly shows that the new phase has a preferred orientation.

The unidentified reflection is not seen in the diffraction scans of poled oriented films when the molecular chains are perpendicular to the applied field. This suggests that for this field-induced phase transformation the dipole moment component along the chain is also important. At the very highest poling field the unidentified reflection decreases in intensity and this suggests that the new phase at very high fields shows a further transformation to a more polar structure.

Initially, the phase II crystallites are unoriented, as is clear from Figure 4; all crystal orientations with respect to the applied field are equally likely. If crystals with a particular orientation (defined by a particular set of three-dimensionsl angular coordinates) show a crystal phase transformation to a new phase, both the new phase and the initial phase (which now has crystals at all orientations except the ones that have transformed) show preferred orientation. This can be seen by comparing Figures 4 and 5. Phase II crystals with the *a* axis close to perpendicular to the film can readily transform to phase IV (which is a polar structure) by a chain reorientation of 180°. If this takes place in our initially unoriented film, the phase IV will have a preferred orientation with the *a* axis close to perpendicular to the film surface. Moreover, the untransformed phase II crystals will be present in all orientations except this one. Figure 5 shows a decrease of intensity in the meridional direction for the (100) reflection and an increase in intensity for the (200) reflection. Figure 2 shows that the (100) intensity (in the reflection mode) decreases sharply from 0.6 to 1.6 MV/cm. It is important to realize that the geometrical arrangement used in the reflection scan entails that the (100) reflection observed originates only from crystals with an *a* axis perpendicular to the film. In the same scan, the (200) reflection shows an increase. In the transmission mode, the (100) reflection originates chiefly from crystals with the *a* axis in the plane of the film, and it can be seen that from 0.6 to 1.6 MV/cm there is little change. The principal difference between phase II and phase IV is that in phase IV the structure factor for the (100) reflection is quite small, while for the (200) reflection, the structure factor is increased. Figure 4 shows an increase in intensity for the (200) reflection over an arc ~30° to either side of the meridian, suggesting that phase II crystals within this angular range of orientation with respect to the applied field transform to phase IV. Thus the phase IV formed has preferred orientation and the phase II remaining also has preferred orientation. However, since phases II and IV have all reflections in common, only some of which differ in intensity, most of the Debye–Scherrer rings will be complete, both phase II and phase IV crystals contributing to intensity.

Since the response of crystallites making different angles with respect to the applied field is likely to be different, to analyze our X-ray data we classified crystals as belonging to one of four different groups: (a) phase II crystals with the molecular chains in the plane of the film and the *a* axes close to perpendicular to the film surface, (b) phase II crystals with the molecular chains in the plane of the film and the *b* axes close to perpendicular to the film surface, (c) phase II crystals with the molecular chains or *c* axes close to perpendicular to the film surface, and (d) phase II crystals with the molecular chains making some angle ϕ ($45° < \phi < 90°$) with respect to the film surface. This classification of crystals was made with a view to examining possible polarization mechanisms and was also implied by the X-ray film and diffractometer geometry used and the reflections observed. As we have already suggested, phase II crystals with the *c* axes in the plane of the film and the *a* axes perpendicular to the film are observed at the meridian position of Figure 6 for the (100) and (200) reflections and from the (100) and (200) reflections from the diffraction scan of Figure 2. Phase II crystals with the *c* axes in the plane of the film and the *b* axes perpendicular to the film are observed at the meridian position of Figures 4 for the (010) reflection and from the (010) reflection in the diffraction scan in Figure 2. Phase II crystals with the molecular chains perpendicular to the film are observed from the (002) reflection at the meridian from Figure 4 and from the (002) reflection in the diffraction scan of Figure 2. Phase II crystals with the molecular chains making a large angle with respect to the perpendicular to the film are seen from (*hkl*) reflections (providing $l > 0$) at the meridional position in Figure 4.

Since the electric field is applied perpendicular to the film surface, we expect crystals making the same angle with respect to the film normal to respond identically. Indeed, the flat-film photograph taken with the incident X-ray beam perpendicular to the film (after the sample had been poled at 3.2 MV/cm) (Figure 7) showed complete symmetry about the film normal. On the other hand, a given set of crystals with a direction in common, $[hkl]^*$, will all contribute intensity at the meridian for the reflection (*hkl*) in an X-ray photograph taken with the incident beam parallel to the film surface and the X-ray film perpendicular to the incident X-ray beam in the front-reflection region, as in the case of Figures 4–6. If we consider other reflections $(h'k'l')$ from the same set of crystals, then the Bragg angle will be satisfied only for a small fraction. Thus these orientation effects caused by phase changes will usually not be observed at nonmeridional locations on the Debye–Scherrer rings. In most cases, the intensity contributed by untransformed crystals (at the same Bragg angle since most reflections are common to phases II, III, and IV) at the nonmeridional position will eclipse the effects caused by the transformed crystals. It was those general considerations that led to the following interpretation of the X-ray results.

(a) Phase II Crystals with *a* Axes Perpendicular to the Film. These crystals have molecular chains in the plane of the film and dipoles either parallel to or opposed to the applied field.

The intensity of the (100) reflection for these crystals decreases at low fields to (0.6–1.6 MV/cm) when other changes are not seen. This appears to be caused by the II → IV transformation for these crystals, first reported for oriented phase II films. If the *a* axes are perpendicular to the film, then the oriented phase IV crystals will be responsible for the residual polarization, giving rise to the linear variation of e_{31} with poling field. A threshold poling field of ~0.6 MV/cm appears necessary to initiate the phase transition, although, of course, we do not know the internal fields. Measurement of the angular range of missing intensity of the (100) phase II reflection suggests that crystals with the *a* axis inclined to the field by an angle $\theta < 30°$, transform.

These crystals do not at higher fields transform to phase III, since the (111) reflection (which does not overlap with any of the phase I, II, or IV reflections) would appear as arcs at either side of the meridian at a Bragg angle 22.5° and this is not observed. Moreover, these crystals do not transform to phase I, since the intense reflections (110) and (200) would appear as arcs to either side of the meridian and at the equator. These phase I reflections would not overlap other reflections and if present would be seen. The (110) phase I reflection observed following the highest poling field (3.2 MV/cm) appears centered at the meridian, and there is no intensity at the equator.

We conclude therefore that crystals with the *a* axis inclined with respect to the field direction ($\theta < 30°$) transform II → IV for poling fields 0.6–2.4 MV/cm but do not show further transformations to other structures at higher fields.

(b) Phase II Crystals with *b* Axes Perpendicular to the Film. These crystals have molecular chains in the plane of the film but in this case the dipole moments are also in the plane of the film, making an angle of 90° with respect to the applied field. The (020) reflection in Figure 2 and the meridian position for the (020) reflection in Figure 5 originate from these crystals. In Figure 5 we see only a small decrease at the meridian and in Figure 2 (which provides a quantitative measure) we see that at fields up to 1.6 MV/cm this reflection is essentially unchanged. If these crystals transformed without dipole rotation II → I, II → III, or II → IV, there would be no increase in the net polarization. In phases III and IV a reflection is observed at the same Bragg angle with approximately the same intensity as the (020) reflection for phase II, so II → III or II → IV transformations could not be observed from this reflection. The intensity of the (100) reflection for phases II and IV is very small and for these crystals is observed in Figure 3 and at the equator in Figure 5. There appears to be no decrease in the (100) reflection at fields up to 1.6 MV/cm. However, it should be remembered that there is a large set of crystals contributing to the intensity of the (100) reflection at those locations

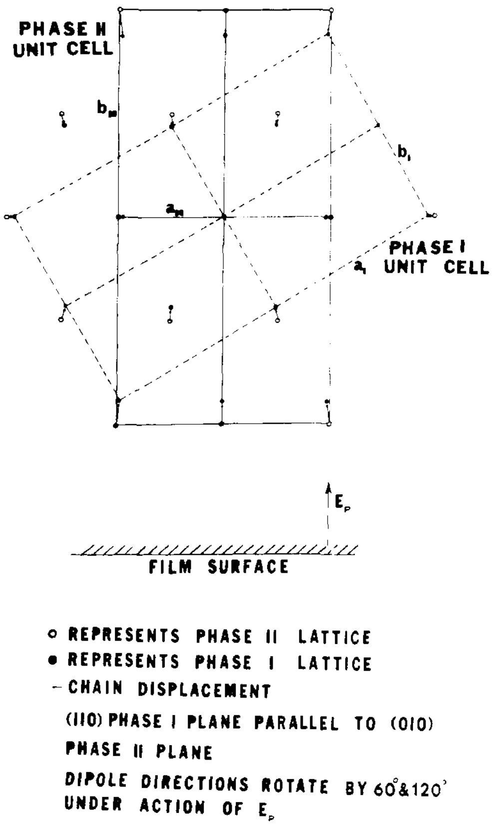

Figure 11. Lattice distortions for the proposed II → I phase transition occurring for crystals with the *b* axis perpendicular to the film surface.

(for example, crystals with the *c* axis perpendicular to the film), and contributions from the particular set under consideration here may be relatively minor.

However, at higher fields ($E_p > 1.6$ MV/cm), the intensity of the (020) reflection in Figure 2 and at the meridian in Figure 6 is dramatically decreased. As we have explained, a transformation without rotation of II to III or II to IV would not give this result and, moreover, would not give rise to an increased residual polarization. A transformation of II to I without rotation for these crystals would lead to disappearance of the (020) reflection at the meridian in Figures 5 and 6, but again since there would be no increase in polarization associated with this transformation for these crystals, it seems unlikely. Moreover, the decrease in the (020) intensity does not appear to be associated with the appearance of the new reflection at 23.7° (which we attribute to phase VI) since this new reflection finally decreases at the highest fields while the (020) intensity continues to decrease (Figures 5 and 6).

In order to achieve a change in residual polarization, a rotation of the dipole moment out of the plane of the film is required. Moreover, a phase transition to a polar phase such as II → III, II → IV, or II → I must occur. A transition to phase I at the highest fields is seen in Figure 2 and Figure 6. The orientation of the transformed crystals, (110) planes parallel to the surface, is surprising since the dipoles are *inclined* by an angle α ($\sim 30°$) to the field direction. However, as we have explained previously, if the dipoles for phase I are in the field direction, the (200) reflection would be seen in the diffraction scan in Figure 3 and on the equator in Figure 6. This was not observed.

A possible mechanism that would explain this is suggested by Figure 11. The phase II chain packing is close to hexagonal. Although the unit cell has monoclinic symmetry, it is metrically orthorhombic and the angles between the diagonals in the *ab* projection is 55°. In Figure 11, a phase II crystal with the *b* axis perpendicular to the film surface is shown. The lattice is approximately hexagonal ($a \sim 5.02$ Å). On the same lattice a suggested phase I unit cell is drawn. Although the phase I cell is orthorhombic, the molecular packing is also close to hexagonal and in fact all the reflections from the phase I structure can be indexed on a hexagonal lattice with $a = 4.90$ Å. We notice an interesting and special geometrical relation between the phase II and phase I lattices. The (110) planes for the derived phase I cell are perpendicular to the *b* axis for the phase II cell; that is, the (110) planes for phase I are parallel to the crystal surface. This is in agreement with the X-ray data.

We suggest then that the new oriented phase I crystals are produced by a transformation of phase II crystals with the *b* axis parallel to the field direction and a change of conformation from TGTG′ to an all-trans conformation, with the final phase I lattice, however, bearing the previously described geometrical relation to the original phase II lattice. The volume fraction of crystals having the orientation required for this transition is too small to give rise to a measurable change in film thickness.

An alternative polarization mechanism utilizing a II → IV transition can be postulated. This transition could be accompanied by chain rotations of 90° so that the new phase IV crystals are oriented with dipoles parallel to the field direction.[18] No new reflections should be observed. The intensity of the (100) reflection associated with the new phase IV crystals would be very small and would not cause any observable change. A small continuous increase in the intensity of the (200) reflection in Figure 2 at the highest fields is observed. This mechanism would entail considerable repacking motions (akin to a recrystallization) and, moreover, would not explain the presence of the oriented phase I crystals.

(c) Phase II Crystals with Molecular Chains (or *c* Axes) Perpendicular to the Plane of the Film. As we have previously explained, the phase II chain conformation has large dipole moment components perpendicular and parallel to the chain direction, but the net dipole moment of a phase II crystal is zero, since dipoles in neighboring chains are opposed. Rotations about the chain axes will not lower the potential energy with respect to the applied field for the crystals considered here, so we would not anticipate a II → IV, II → III, or II → I transformation for these crystals. In fact, since the dipole moment component along the chain is less for some of these phases, the effect would be an increase in energy.

The (002) reflection in the meridional position of Figures 4–6 and the (002) diffraction peak in Figure 2 after poling at the highest field do show a significant change. From Figure 6 we observe that the (002) reflection appears broader at the meridian than at the equatorial position. Furthermore, comparison of the X-ray scans of Figures 2 and 3 for the samples poled at the very highest field shows a distinct difference in the (002) peak. In Figure 2 we notice that the intensity is reduced and there appear to be two peaks separated by a Bragg angle of $\Delta(2\theta) \sim 0.7°$. The initial (002) peak (quite broad) seems to have separated into two smaller peaks separated by a small Bragg angle.

A II → VI transformation would not give rise to a meridional reflection for these crystals unless it were an (001) reflection. The unidentified reflection with Bragg angle $2\theta = 23.7°$ does not correspond to any simple conformational change, and in any event such a transition would give rise to a decrease in the phase II (002) reflection at the meridian, as we observed for the II → IV transition and the (100) phase II reflection.

A final possibility exists that the chains change their sense to a parallel packing (parallel phase II or parallel phase IV), giving a net polarization in the chain direction. The antiparallel and parallel structures are very similar for phase II, with similar molecular packing and calculated structure factors. The antiparallel structure provides a plausible explanation for the metrically orthorhombic dimensions observed. The changes in the intensities of the reflection entailed by this transformation are small enough so that it cannot be ruled out. Such a transition could occur not, of course, by an end-over-end rotation but by a series of conformational changes. Small changes in the unit cell parameters might then occur. If the cell angles are no longer exactly 90°, a small change in the *d* spacing of the (001) reflection might take place and be the basis for the changes observed in the (002) reflection at the meridian. We conclude that a transition to an all-parallel phase II or phase IV structure with the polarity directed along the chain direction may have occurred at the highest poling field.

(d) Phase II Crystals with the Molecular Chains Making Some Angle ($45 < \phi < 90°$) with respect to the Film Surface. The (021) reflection begins to decrease at 2.4 MV/cm in the meridional position in Figure 5 and in the reflection-mode diffraction scan (Figure 2) and after poling at 3.2 MV/cm has decreased substantially. This reflection originates from crystals with the *c* axis at 45° to the film normal. We assume these crystals are also undergoing a crystal transition to a polar phase. Since the behavior parallels the behavior of the (020) reflection, a likely explanation is that a crystal transformation II $\rightarrow$ I occurs for these crystals also. The (110) reflection of the new phase I is not in the correct orientation for diffraction in either Figure 2 or Figures 5 and 6.

A reflection at a Bragg angle of 23.7° appears after poling at 2.4 MV/cm. As we have already observed, since this cannot be indexed on any of the known crystal structures, it must arise from a new crystal form. After poling at 2.4 MV/cm, it appears as the third most intense reflection of the pattern in Figures 2 and 5. Figure 5 shows the orientation of the new phase VI very clearly as an arc on the meridian. This reflection is not observed for biaxially oriented films when the *c* axis is in the plane of the film, so the new phase VI crystals do not originate from crystals with this orientation. We have already pointed out that the changes taking place in the (002) phase II reflection at the highest poling field, originating from crystals with the *c* axis perpendicular to the film, are not associated with the appearance of this new reflection. Thus the crystals of the new phase originate from crystals with molecular chains making some large angle with both the film plane and the film normal. At the highest field, 3.2 MV/cm, this new reflection is reduced in intensity somewhat, which suggests that at higher fields, these crystals transform to phase I. It is this feature that enables us to assume that the decrease in the (021) reflection is not associated directly with the increase in phase VI crystals. Since in any crystal transition we assume that the direction of the molecular chains is unchanged, it would appear that the new reflection is indexed (*hkl*), where *l* is not zero and either *h* or *k* is also not zero. The new phase must be polar. A high crystal polarity for crystals with *c* axes inclined to the field can be achieved if the net dipole moment associated with the chain is inclined to the chain. This is, for example, true for phases II, III, and IV. It is the antiparallel packing of these structures that leads to the zero dipole moment component in the chain direction.

The (111) reflection of phase II after poling at 2.4 and 3.2 MV/cm can be seen as a complete ring, with, however, a high intensity at the meridian. If some crystals with the (111) direction perpendicular to the film (chains 45° to the film normal) transformed to parallel phase II or parallel phase IV, a net increase in remnant polarization would result. If the unit cell dimensions of parallel phase II or parallel phase IV are similar to those of phase II or phase IV cells, no marked change in the (111) reflection would be anticipated apart from a slight broadening and a change in intensity associated with the structure factors of the new phase.

The X-ray data for the unpoled oriented films (Figure 8) show the presence of a small fraction of oriented phase I crystals. The X-ray data taken for the poled oriented films (Figures 9 and 10) do not show the same structural changes as those occurring in the unoriented films. Careful examination of Figure 9 reveals a weak reflection arced on the meridian at the same Bragg angle as the unidentified VI reflection. In addition, a second stronger reflection arced at the meridian at the Bragg angle for the phase III (111) reflection can be observed. The observation that the unidentified reflection is weak for the oriented poled films is consistent with our suggestion that this reflection originates from crystals *c* axes making some large angle to the film surface. The broadening and splitting of the (002) reflection observed at the meridian for the unoriented films poled at the highest fields are also not observed for the oriented films. It is interesting to note that following the highest poling field, the ratio of the (002) phase II intensity to the (001) phase I intensity is greatly reduced, and it appears from Figure 10 from the (002) phase II reflection that the phase II crystals are no longer oriented. This would be the case if most of the phase II crystals with molecular chains in the plane of the film transformed to phase I, whereas other unoriented crystals remained unchanged.

All the other observed changes can be interpreted on the basis of the phase II to phase IV transition previously discussed.

In summary, we conclude that a number of polarization mechanisms can combine for the case of poled unoriented phase II films (if high poling fields are used) to give residual polarizations as high as that observed for oriented films. These are the following:

(1) Crystals with the *a* axis within 30° of the film normal undergo II $\rightarrow$ IV transition. At room temperature, the threshold poling field is 0.6 MV/cm. Presumably, this is for crystals with axes exactly perpendicular to the film, larger fields being required for crystals inclined to the normal.

(2) Crystals with the *b* axis perpendicular to the film undergo a transition to a polar phase at fields above 2.4 MV/cm. We believe the new phase is phase I with a unique lattice orientation to the initial phase II crystals. However, a mechanism consisting of chain rotations of 90° to give a transformation to phase IV crystals with the *a* axis perpendicular to the film surface is also possible.

(3) Crystals with molecular chains at 45° to the film normal and the *a* axis in the plane of the film transform to phase I.

(4) Crystals with molecular chains making some angle ϕ with respect to the film surfaces, $45° < \phi < 90°$, transform to a new polar phase.

(5) The new polar phase has a dipole component in the chain direction as well as a component perpendicular to the chain, and after the phase transition the net dipole moment is close to the field direction.

(6) Phase II crystals with molecular chains perpendicular to the film transform to an all-parallel phase II or phase IV structure.

In future studies, these conclusions will be examined using complete pole figure analysis. However, these preliminary studies were necessary since pole figure analysis cannot be carried out in an unambiguous way for samples containing different crystal structures with many reflections in common. We are also poling films with special orientations, for example, with molecular chains perpendicular to the plane of the film, to provide cases where a unique polarization mechanism can be isolated.

Acknowledgment. This work was supported in part by the Office of Naval Research.

Registry No. PVF_2, 24937-79-9.

References and Notes

(1) Newman, B. A.; Yoon, C. H.; Pae, K. D.; Scheinbeim, J. I. *J. Appl. Phys.* **1979**, *50*, 6095.
(2) Bachmann, M.; Gordon, W. L.; Weinhold, S.; Lando, J. B. *J. Appl. Phys.* **1980**, *51*, 5095.
(3) Broadhurst, M. G.; Davis, G. T.; McKinney, J. E.; Collins, R. E. *J. Appl. Phys.* **1978**, *49*, 4992.
(4) Southgate, P. D. *Appl. Phys. Lett.* **1976**, *28*, 250.
(5) Das-Gupta, D. K.; Doughty, K. *Appl. Phys. Lett.* **1977**, *31*, 585.
(6) Das-Gupta, D. K.; Doughty, K. *J. Appl. Phys.* **1978**, *49*, 4601.
(7) McKinney, J. E.; Davis, G. T. *Org. Coat. Plast. Chem.* **1978**, *38*, 271.
(8) Davis, G. T.; McKinney, J. E.; Broadhurst, M. G.; Roth, S. C. *J. Appl. Phys.* **1978**, *49*, 4998.
(9) Servet, B.; Rault, J. *J. Phys. (Paris)* **1979**, *40*, 1145.
(10) Hasegawa, R.; Kobayashi, M.; Tadokoro, H. *Polym. J.* **1972**, *3*, 591.
(11) Doll, W. W.; Lando, J. B. *J. Macromol. Sci., Phys.* **1968**, *B2* (2), 219.
(12) Lando, J. B.; Olf, H. G.; Peterlin, A. *J. Polym. Sci., Part A-1* **1966**, *4*, 941.
(13) Contilli, G.; Zerbi, G. *Spectrochim Acta, Part A* **1967**, *23A*, 2216.
(14) Kobayashi, M.; Tashahiro, K.; Tadokoro, H. *Macromolecules* **1975**, *8*, 158.
(15) Doll, W. W.; Lando, J. B. *J. Macromol. Sci., Phys.* **1970**, *B4* (2), 309.
(16) Weinhold, S.; Litt, M. H.; Lando, J. B. *Macromolecules* **1980**, *13*, 1178.
(17) Takahashi, Y.; Tadokoro, H. *Macromolecules* **1980**, *13*, 1178.
(18) Buchman, P. *Ferroelectrics* **1973**, *5*, 39.
(19) Tamura, M.; Ogasawana, K.; Ono, N.; Hagiwana, S. *J. Appl. Phys.* **1974**, *45*, 3768.
(20) Oshiki, M.; Fukada, E. *J. Mater. Sci.* **1975**, *10*, 1.
(21) Scheinbeim, J. I.; Yoon, C. H.; Pae, K. D.; Newman, B. A. *J. Appl. Phys.* **1980**, *51*, 5156.
(22) Scheinbeim, J. I.; Yoon, C. H.; Pae, K. D.; Newman, B. A. *J. Polym. Sci., Polym. Phys. Ed.* **1980**, *18*, 2271.
(23) Das-Gupta, D. K.; Doughty, K. *J. Appl. Phys.* **1978**, *11*, 2415.
(24) Bachmann, M.; Lando, J. B. *Macromolecules* **1981**, *14*, 40.
(25) Lovinger, A. J. *Macromolecules* **1981**, *14*, 322.

Light Beating Spectroscopy of Branched Poly(propylene glycol)

Chin-Hsien Wang*
Department of Chemistry, University of Utah, Salt Lake City, Utah 84112
George Fytas and Thomas Dorfmüller
Faculty of Chemistry, University of Bielefeld, 4800 Bielefeld 1, West Germany.
Received May 6, 1982

ABSTRACT: Linear and trifunctional star polymers of propylene glycol with about the same molecular weight ($\simeq$3000) were studied by the laser light beating spectroscopic technique. Macroscopic shear viscosity measurements were also carried out. The time correlation functions for the density fluctuation were determined for both the linear and the branched polymers. The time correlation functions display a nonexponential shape. The results show that although the two polymers have about the same viscosity over the temperature range between −30 and +25 °C, the relaxation time for branched poly(propylene glycol) is several times longer than that of linear poly(propylene glycol), in contrast to dielectric relaxation data, which show that linear and branched polymers have nearly identical dielectric behavior.

Introduction

Studies of the dynamics of segmental motion of a bulk polymer liquid by the laser light beating spectroscopic technique are of considerable current research interest. The dynamic light scattering data have provided very useful insight into the physical processes associated with the glass transition processes.

In a recent article, we reported the results of a comprehensive laser light beating spectroscopic study of linear poly(propylene glycol) (PPG).[1] The study deals with the measurements of the homodyne intensity time correlations of the scattered field as a function of temperature for linear PPG of different molecular weights. The time correlation functions for the fluctuations of the polarizability density which give rise to light scattering were extracted from the measured homodyne intensity time correlation function. The important results found are as follows: (1) Over the time scale from 1 to 10^{-6} s, the time correlation functions from both VV and VH scattering geometries are independent of the scattering angle. The mean relaxation times derived from the VV and VH time correlation functions are, however, nearly equal. (2) The temperature dependence of the mean relaxation times follows the Vogel–WLF equation but not the Arrhenius equation. (3) The mean relaxation times for all polymers depend only on temperature and not on the macroscopic shear viscosity associated with the difference in the molecular weight for different polymers. When the mean relaxation time is scaled according to the "segment viscosity", all temperature-dependent data from polymers of different molecular weights fall on a master curve. This result suggests that the localized side-group orientation and the backbone motion associated with the conformational flip are the mechanisms responsible for the dynamic light scattering in PPG.

In this paper, we report the result of the effects due to branching on the homodyne time correlation function, keeping the molecular weight of PPG fixed. This complements the result of a similar study using the dielectric relaxation technique by Stockmayer and Burke.[2] These

0024-9297/83/2216-0068$01.50/0